Synergistic effect of Au-COFs nanosheets and artificial peroxidase Au@ZIF-8(NiPd)) rhombic dodecahedra for signal amplification for biomarkers detection

Tingting Zhang[a], Yu Song[a], Yue Xing[a], Yue Gu[a], Xiaoyi Yan[a], He Liu[a], Nannan Lu[a], Haixin Xu[a], Zhiqian Xu[a], Zhiquan Zhang[a]*, Ming Yang[b*]

[a] College of Chemistry, Jilin University, Changchun 130012, China

[b] Department of Physiology, College of Basic Medical Sciences, Jilin University, Changchun 130021, China

[*] Corresponding author. Tel: +86-431-85168352-7; Fax: +86-431-85168399

E-mail address: zzq@jlu.edu.cn (Z. Zhang); yangming1967@163.com(M. Yang)

Reagents and materials.

Zinc nitrate hexahydrate ($Zn(NO_3)_2 \cdot 6H_2O$), 2-Methylimidazole, o-phenylenediamine (OPD), trisodium citrate were the products of Sinopharm Chemical Reagent, Co. 3, 3', 5, 5'-tetramethylbenzidine (TMB), 2, 2'-azino-bis (3-ethylbenzothiazoline-6-sulfonic acid) (ABTS), palladium chloride, tetrachloroauric acid ($HAuCl_4 \cdot 4H_2O$), TB, polyvinylpyrrolidone (PVP, Mw~8000), 1,4-benzenediboronic acid (BDBA), 1,4-dioxane, mesitylene were purchased from Sigma-Aldrich. TBA (1 and 2): 5′-NH_2-$(CH_2)_6$-GGT TGG TGT GGT TGG-3′ were obtained from Sangon Biotech Co., Ltd, China. The human serum was acquired from The First Hospital of Jilin University, Changchun. 20 mM Tris-HCL buffer (pH = 7.0) containing 140 mM NaCl, 5 mM KCl, 1 mM $CaCl_2$, and 1 mM $MgCl_2$ was employed to prepared aptamers solutions. The 10 mM phosphate buffer solution (PBS, pH = 7.0) was used to prepare TB solutions and utilized as detection buffer. Ultrapure water was used throughout the study.

Apparatus.

The nanomaterial was characterized by Scanning electron microscopy (SEM, JEOL JSM 6700F), Transmission electron microscopy (TEM, Philips-FEI Tecnai G2S-Twin), Scanning TEM-energy-dispersive X-ray spectroscopy (STEM-EDS, Philips-FEI Tecnai G2S-Twin), Fourier transform infrared spectroscopy (FTIR, Nicolet Impact 410), UV–vis absorption spectra (Varian GBC Cintra 10 e UV–vis spectrometer), X-ray diffraction (XRD, Rigaku D/Max 2550 X-ray diffractometer).

Electrochemical measurements were carried out on a CHI 920C electrochemical

workstation (Shanghai Chenhua Instrument Co., China). Working electrode: bare glassy carbon electrode (GCE, 3 mm in diameter). Reference electrode: saturated calomel electrode (SCE). Counter electrode: platinum wire.

Experimental Section

Steady-State kinetic analysis of Au@ZIF-8(NiPd) as peroxidase mimetics:

Kinetic experiments were conducted referring to the related literatures[1, 2] in 0.2 M NaOAc buffer solution (pH 4.5) containing 10 μg mL^{-1} Au@ZIF-8(NiPd), 0.5 mM TMB, and different concentrations of H_2O_2. For simplicity, the mixed solutions were incubated at room temperature for 3 min and then used for absorbance measurement at wavelength 652 nm. The Michaelis-Menten constant was calculated using a Lineweaver-Burk plot: 1/V = Km/Vm (1/[S] + 1/Km), where V is the initial velocity, Vm is the maximal reaction velocity, [S] corresponds to the substrate concentration, and Km is the Michaelis-Menten constant.

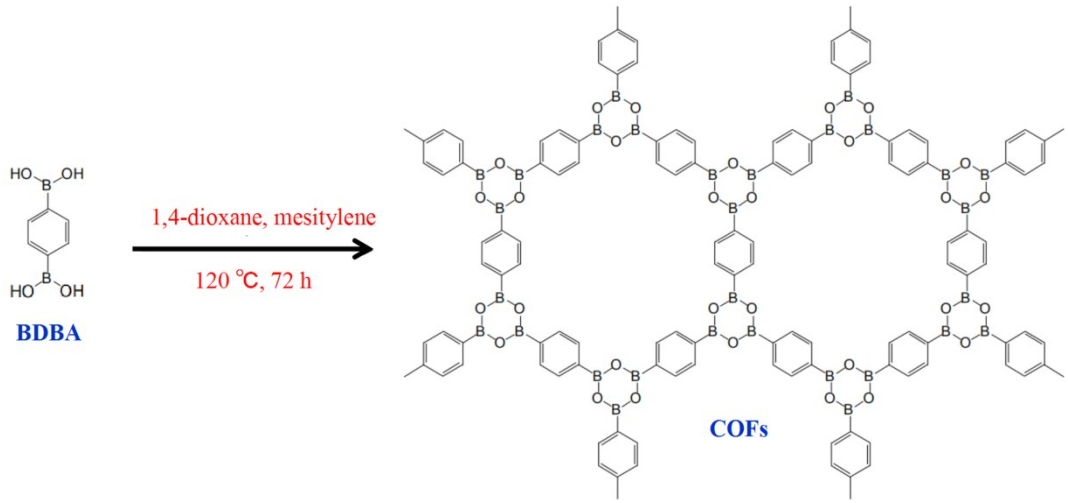

Scheme S1 Preparation of COFs via a solvothermal process.

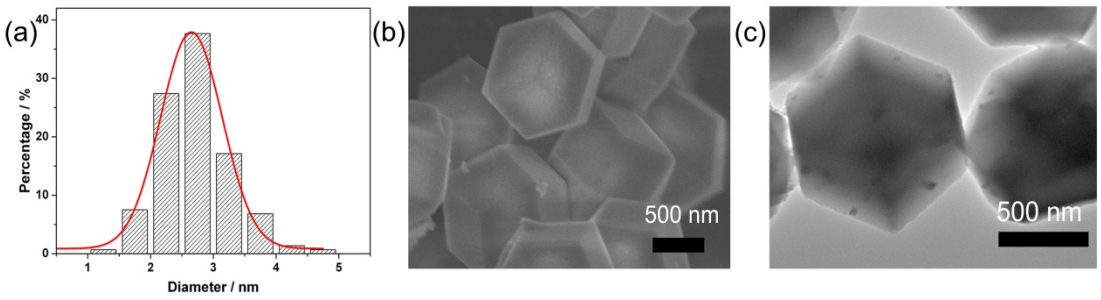

Figure S1. (a) The size distribution of NiPdNPs. (b) SEM image of ZIF-8(NiPd). (c) TEM image of ZIF-8(NiPd).

The steady-state kinetic parameters were verified by changing the concentration of H_2O_2. The value ε = 39000 M^{-1} cm^{-1} (at 652 nm) for the oxidized product of TMB was used here to obtain the corresponding concentration term from the absorbance data. Typical Michaelis–Menten curves were shown in Figure S2. The Vmax and Km calculated using Lineweaver–Burk plot were given in Table S1. Compared with horseradish peroxidase (HRP), the Km value of Au@ZIF-8(NiPd) with H_2O_2 as the substrate is lower, indicating the higher catalytic activity of Au@ZIF-8(NiPd).

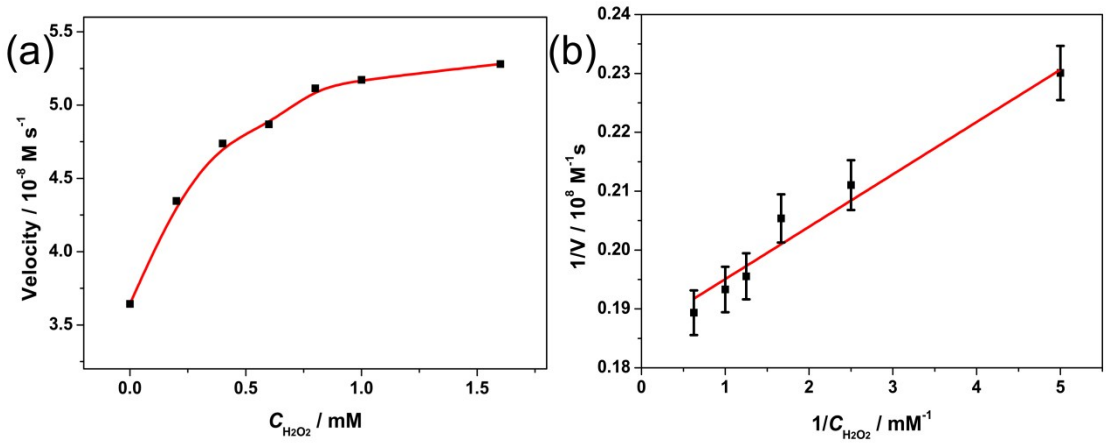

Figure S2. Steady-state kinetic assay of Au@ZIF-8(NiPd). (b) Double reciprocal plots of activity of Au@ZIF-8(NiPd). Experimental conditions: 10 μg mL^{-1} Au@ZIF-8(NiPd) in pH 4.5 NaOAc buffer solution containing 0.5 mM TMB.

Table S1. Comparison of the apparent Michaelis-Menten constant (Km) and maximum reaction rate (Vm).

Catalyst	Km (mM)	Vm (10^{-8} M s^{-1})	Ref
	H_2O_2	H_2O_2	
HRP	3.7	8.71	[3]
Pd-Ir cubes	340	5.1	[4]
ZIF-8(NiPd)	0.89	7.09	[5]
Au@ZIF-8(NiPd)	0.049	5.39	This work

Optimization of the detection conditions.

As shown in Figure S3, the current change reaches a maximum at 10 μL of COFs suspension, when the volume increases to more than 10 μL, it would lead to the formation of thick film that hinders the electron transfer and weakens electrochemical response. Therefore, 10μL of COFs suspension is selected as the optimum.

The electrodeposition time of AuNPs controls the quantity of AuNPs, which influence the electron transfer and the anchoring of TBA 1. As shown, the electrochemical response improves gradually from 10 to 40 s and attains the maximum at 40 s, and then decreases. The long electrodeposition time causes the excess of AuNPs, which reduces electrochemical response. Hence, 40 s is the optimal electrodeposition time.

With respect to the effect of the incubation time of TB, different incubation time was inspected. The electrochemical signal increases rapidly with the increasing of incubation time and remains steady at 60 min, indicating the binding of TB is saturated. Consequently, 60 min is chosen as the optimal incubation time.

The effects of the volume of tracer labels were also investigated. Various volumes of tracer labels were casted onto the electrodes, and 20 μL tracer labels achieve the best electrochemical performance. Hence, 20 μL is selected as the optimum.

To investigate the effect of H_2O_2 concentration, the aptasensor was used to detect TB with different concentration of H_2O_2 as the signal molecule. As shown in Figure S3e, the peak current increased with the increasing concentration of H_2O_2, and become stable at 5 mM, suggesting the highest electrocatalytic efficiency at this point. Therefore, 5 mM H_2O_2 was selected throughout the whole experiment.

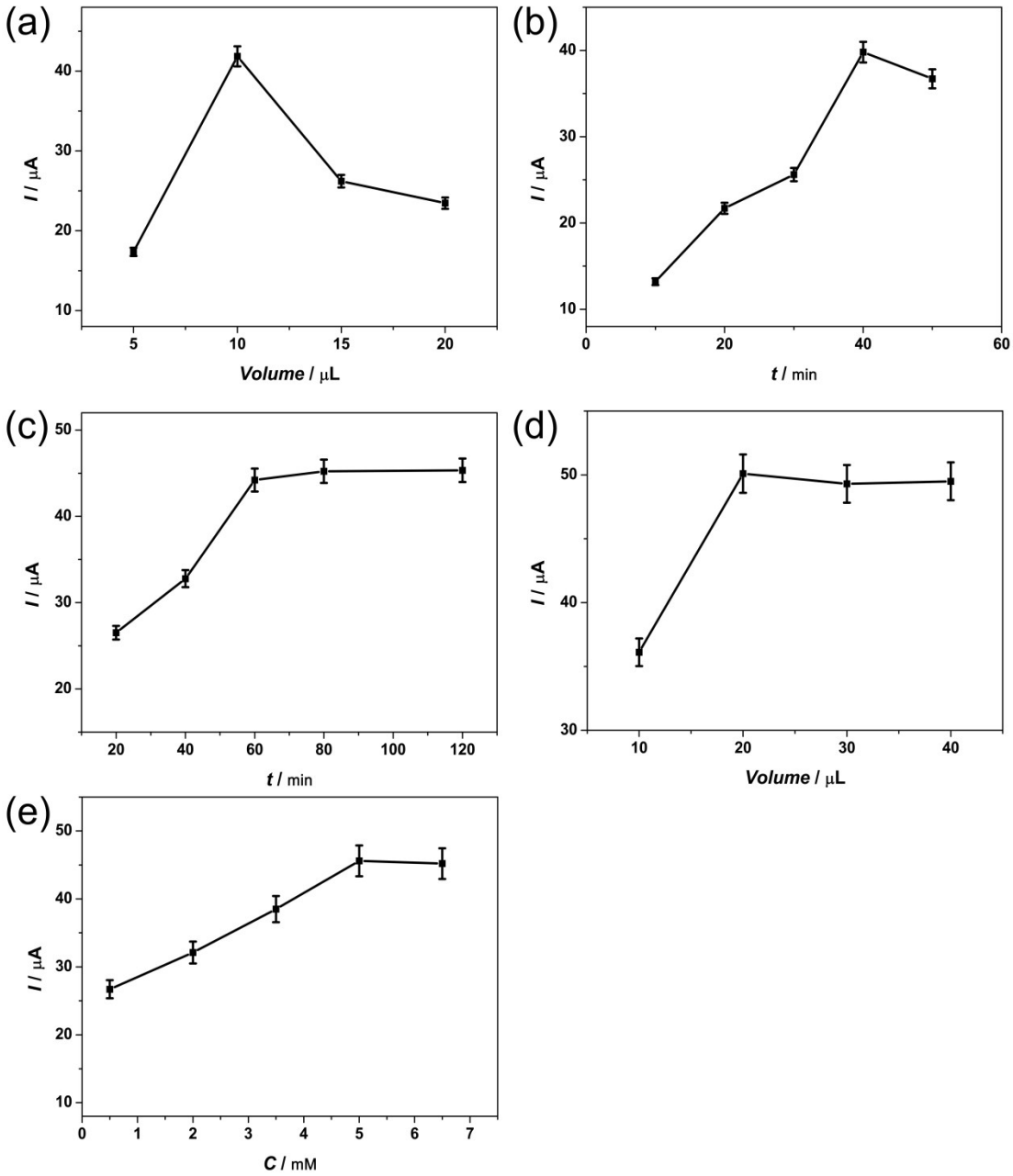

Figure S3. Effects of (a) the volume of the COFs nanosheets suspension, (b) deposition time of AuNPs, (c) the incubation time of TB, (d) the volume of the TBA 2–Au@ZIF-8(NiPd) (tracer labels), (e) the concentration of H_2O_2.

Table S2 Comparison of previous works for TB detection.

Analytical method	Linear range	Detection limit (fM)	Ref
impedance	2−14 ng mL^{-1}	58000	6
different pulse	1 pM −30 nM	320	7
different pulse	0.1 pM−80 nM	32	8
chronoamperometry	0.1 pM−20 nM	23	9
chronoamperometry	0.1 pM−20 nM	15	This work

References

1. J. Wu, X. Wang, Q. Wang, Z. Lou, S. Li, Y. Zhu, L. Qin and H. Wei, *Chem Soc Rev*, 2019, **48**, 1004-1076.
2. Q. Wang, L. Zhang, C. Shang, Z. Zhang and S. Dong, *Chem Commun*, 2016, **52**, 5410-5413.
3. L. Gao, J. Zhuang, L. Nie, J. Zhang, Y. Zhang, N. Gu, T. Wang, J. Feng, D. Yang, S. Perrett and X. Yan, *Nat. Nanotechnol.*, 2007, **2**, 577.
4. X. Xia, J. Zhang, N. Lu, M. J. Kim, K. Ghale, Y. Xu, E. McKenzie, J. Liu and H. Ye, *ACS Nano*, 2015, **9**, 9994-10004.
5. Q. Wang, X. Zhang, L. Huang, Z. Zhang and S. Dong, *Angewandte Chemie-International Edition*, 2017, **56**, 16082-16085.
6. V. Urbanová, K. Jayaramulu, A. Schneemann, Š. Kment, R. A. Fischer and R. Zbořil, *ACS Appl Mater Interfaces*, 2018, **10**, 41089-41097.
7. X. Yang, J. Lv, Z. Yang, R. Yuan and Y. Chai, *Anal Chem*, 2017, **89**, 11636-11640.
8. Y.-C. Zhou, X.-X. Ran, A.-Y. Chen, Y.-Q. Chai, R. Yuan and Y. Zhuo, *Anal Chem*, 2018, **90**, 9109-9116.
9. Y. Liu, D. Wang, L. Xu, H. Hou and T. You, *Biosens Bioelectron*, 2011, **26**, 4585-4590.